Tsuji A, Wada H, Matsumoto T, Abe Y, Ota S, Yamada N, Sugiyama T, Sudo A, Onishi K, Nakatani K, Uchida A, Ito M, Suzuki K, Nobori T	Elevated levels of soluble fibrin in patients with venous thromboembolism.	Int J Hematol	88	448-453	2008
Ota S, Wada H, Abe Y, Yamada E, Sakaguchi A, Nishioka J, Hatada T, Ishikura K, Yamada N, Sudo A, Uchida A, Nobori T	Elevated levels of prothrombin fragment 1+2 indicate high risk of thrombosis.	Clinical and Applied Thrombosis/Hemostasis	14	279-285	2008
Fujimoto N, Onishi K, Dohi K, Tanabe M, Kurita T, Takamura T, Yamada N, Nobori T, Ito M	Hemodynamic characteristics of patients with diastolic heart failure and hypertension.	Hypertens Res	31	1727-1735	2008
Nomura H, Wada H, Mizuno T, Katayama N, Abe Y, Noda M, Nakatani K, Matsumoto T, Ota S, Yamada N, Sudo A, Uchida A, Nobori T	Negative predictive value of D: -dimer for diagnosis of venous thromboembolism.	Int J Hematol	87	250-255	2008
Kato S, Onishi K, Yamanaka T,	Exaggerated Hypertensive Response to Exercise in	Hypertension Research	31	679-684	2008

Takamura T, Dohi K, Yamada N, Wada H, Nobori T, Ito M	Patients with Diastolic Heart Failure.				
Dohi K, Onishi K, Gorcsan J, Lopez-Candales A, Takamura T, Ota S, Yamada N, Ito M	Role of radial strain and displacement imaging to quantify wall motion dyssynchrony in patients with left ventricular mechanical dyssynchrony and chronic right ventricular pressure overload.	Am J Cardiol	101	12061211	2008
Ota S, Yamada N, Tsuji A, Ishikura K, Nakamura M, Isaka N, Ito M	The Günther-Tulip retrievable IVC filter: clinical experience in 118 consecutive patients.	Circ J	72	287-292	2008
Iwasaki H, Okamoto R, Kato S, Konishi K, Mizutani H, Yamada N, Isaka N, Nakano T, Ito M	High glucose induces plasminogen activator inhibitor-1 expression through Rho/ Rho-kinase-mediated NF-kB activation in bovine aortic endothelial cells.	Atherosclerosis	196	22-28	2008
Uemura M, Fujimura Y, Matsumoto M, Ishizashi H, Kato S, Matsuyama T, Isonishi A, Ishikawa M, Yagita M, Morioka C, Yoshiji H, Tsujimoto T, Kurumatani N,	Comprehensive analysis of ADAMTS13 in patients with liver cirrhosis.	Thromb Haemost	99	1019-1029	2008

Fukui H.					
Shida S, Nishio K, Sugimoto M, Mizuno T, Hamada M, Kato S, Matsumoto M, Okuchi K, Fujimura Y, Yoshioka A.	Functional imaging of shear-dependent activity of ADAMTS13 in regulating mural thrombis growth under whole blood flow conditions.	Blood	111	1295-1298	2008
Kokame K, Aoyama Y, Matsumoto M, Fujimura Y, Miyata T.	Inherited and *de novo* mutations of *ADAMTS13* in a patient with Upahaw-Schulman syndrome.	J Thromb Haemost	6	213-215	2008
Horii M, Uemura S, Uemura M, Matsumoto M, Ishizashi H, Imagawa K, Iwama H, Takeda Y, Kawata H, Nakajima T, Fujimura Y, Saito Y.	Acute Myocardial Infarction as a Systemic Prothrombotic Condition Evidenced by Increased von Willebrand Factor Protein Over ADAMTS13 Activity in Coronary and Systemic Circulation.	Heart and Vessels	23	301-307	2008
Morioka C, Uemura M, Matsuyama T, Matsumoto M, Kato S, Ishikawa M, Ishizashi H, Fujimoto M, Sawai M, Yoshida M, Mitoro A, Yamao J,	Plasma ADAMTS13 activity parallels the APACHE II score, reflecting an early prognostic indicator for patients with severe acute pancreatitis.	Scand J Gastroenterol	43	1387-1396	2008

Tsujimoto T, Yoshiji H, Urizono Y, Hata M, Nishio K, Okuchi K, Fujimura Y, Fukui H.					
Uemura M, Fujimura Y, Matsuyama T, Matsumoto M, Ishikawa M, Ishizashi H, Tsujimoto T, Yoshiji H, Fukui H.	Potential roles of ADAMTS13 in the development of alcoholic hepatitis.	Current Drug Abuse Reviews	75	S20-S24	2009
Zakarija A, Kwaan HC, Moake JL, Bandarenko N, Pandey DK, Mckoy JM, Yarnold PR, Raisch DW, Winters JL, Raife TJ, Cursio JF, Luu TH, Richey EA, Fisher MJ, Ortel TL, Tallman MS, Zheng XL, Matsumoto M, Fujimura Y, Bennett C.	Ticlopidine- and clopidogrel- associated thrombotic thrombocytopenic purpura (TTP): review of clinical, laboratory, epidemiological, and pharmacovigilance findings (1989-2008).	Kidney Int	75	S20-S24	2009
Fujimura Y,Matsumoto M, Kokame K, Isonishi A,	Pregnancy-induced thrombocytopenia and thrombotic microangiopathy in	Br J Haematol	144	742-754	2009

Soejima K, Akiyama N, Tomiyama J, Kazuhiko Natori K, Kuranishi Y, Imamura Y, Inoue N, Higasa S, Seike M, Kozuka T, Hara M, Wada H, Murata M, Ikeda Y, Miyata T, George JN.	Upshaw-Schulman syndrome: Clinical observations and *ADAMTS13* gene analysis in nine patients representing six families.				

著者名	論文タイトル名	発表誌名	巻号	ページ	出版年
小嶋哲人	血栓性素因としてのATとPC異常	日本検査血液学会雑誌	9(3)	365-370	2008
川崎富夫	学会セッションのテーマ変遷から見た医療水準-静脈血栓症における医療訴訟の検討-	日本血管外科学会雑誌	17(1)	7-12	2008
川崎富夫	(判例研究) 肺塞栓症予防対策における注意義務違反-医療水準とｶﾞｲﾄﾞﾗｲﾝ-	L&T	40	75-83	2008
辻　肇	抗凝固療法．未分画ヘパリンと低分子ヘパリン	CLINICIAN	55(3)	365-368	2008
辻　肇	血栓止血の臨床．ヘパリン類の適正使用	血栓止血誌	19(2)	187-190	2008
辻　肇	血小板・血栓止血の管理-薬物療法．ヘパリン・低分子ヘパリン	救急・集中治療	20(5-6)	747-752	2008
辻　肇	内科診療ガイドライン活用法．播種性血管内凝固症候群（ＤＩＣ）	内科	102(6)	1424-1429	2008
倉田義之	特発性血小板減少性紫斑病診断の進歩	日本検査血液学会雑誌	9	388-393	2008
倉田義之	特発性血小板減少性紫斑病	内科	102	1418-1423	2008
冨山佳昭	造血障害に対する免疫抑制療法 特発性血小板減少性紫斑病	血液フロンティア	18	87-93	2008
冨山佳昭	特発性血小板減少性紫斑病	臨床血液	49	14-21	2008
冨山佳昭	抗血小板薬の種類とその作用機序.	Clinician	567	18-22	2008
小林隆夫，中林正雄，石川睦男，池ノ上克，安達知子，前田真	産婦人科血栓症調査結果2001－2005	日産婦新生児血会誌	18(1)	S3-S4	2008
左近賢人，塚本泰司，小林隆夫，藤田悟，川島隆之，	腹部手術後静脈血栓塞栓症予防に対するフォンダパリヌクスの臨床的評価	臨床医薬	24(7)	679-689	2008

門田守人	一間欠的空気圧迫法をベンチマークとした無作為化オープン試験				
小林隆夫	肺血栓塞栓症/深部静脈血栓症(静脈血栓塞栓症)予防ガイドライン	PTM ガイドラインダイジェスト	10	1-2	2008
小林隆夫	産褥期深部静脈血栓症の予防対策は？	臨床婦人科産科	62(4)	428-433	2008
小林隆夫	周産期の静脈血栓塞栓症予防	International Review of Thrombosis	3 (S1)	143-149	2008
小林隆夫	静脈血栓塞栓症の予防および治療の進歩	臨床病理	56(7)	589-599	2008
小林隆夫	深部静脈血栓症の現状と問題点	Angiology Frontier	7(3)	138-144	2008
小林隆夫	静脈血栓症/肺塞栓症の予防ガイドライン：現状と展望	血栓と循環	16 (3)	228-232	2008
小林隆夫	妊産婦の薬物療法. 6. 抗凝固薬	臨床婦人科産科	62 (9)	1189-1193	2008
小林隆夫	婦人科手術における肺血栓塞栓症の予防	産婦人科治療	97(4)	412-419	2008
小林隆夫	婦人科癌と血栓症	血液フロンティア	18 (10)	1575-1584	2008
小林隆夫	婦人科がん診療のリスクマネジメント，静脈血栓塞栓症	産婦人科の実際	57(11)	1794-1804	2008
小林隆夫	肺血栓塞栓症/深部静脈血栓症（静脈血栓塞栓症）の現況と予防対策の展望	県西部浜松医療センター学術誌	2(1)	6-15	2008
小林隆夫	妊娠中の静脈血栓塞栓症	綜合臨床	58 (1)	147-148	2009
小林隆夫	静脈血栓塞栓症の治療戦略	Pharma Medica	27 (1)	13-16	2009
小林隆夫	静脈血栓塞栓症（VTE）の現況	SRL 宝函	29 (2)	20-27	2009
佐久間聖仁，中村真潮，山田典一，伊藤正明，中野	静脈血栓塞栓症の頻度、臨床的特徴	Therapeutic Research	29(5)	639-640	2008

赳，白土邦男，小林隆夫					
榛沢和彦	深部静脈血栓症．新潟県中越地震における肺塞栓症と深部静脈血栓症−災害避難生活を考える	ASAHI medical	4	58-61	2008

研究成果の刊行物・別冊

Novel System Evaluating In Vivo Pathogenicity of Desmoglein 3-Reactive T Cell Clones Using Murine Pemphigus Vulgaris[1]

Hayato Takahashi,* Masayuki Amagai,* Takeji Nishikawa,* Yoshiko Fujii,* Yutaka Kawakami,† and Masataka Kuwana[2‡]

Autoreactive T cells are thought to be involved in the pathogenesis of autoimmune diseases, but evidence for their direct pathogenicity is almost lacking. Herein we established a unique system for evaluating the in vivo pathogenicity of desmoglein 3 (Dsg3)-reactive T cells at a clonal level in a mouse model for pemphigus vulgaris (PV), an autoimmune blistering disease induced by anti-Dsg3 autoantibodies. Dsg3-reactive CD4$^+$ T cell lines generated in vitro were adoptively transferred into Rag-2$^{-/-}$ mice with primed B cells derived from Dsg3-immunized Dsg3$^{-/-}$ mice. Seven of 20 T cell lines induced IgG anti-Dsg3 Ab production and acantholytic blister, a typical disease phenotype, in recipient mice. Comparison of the characteristics between pathogenic and nonpathogenic Dsg3-reactive T cell lines led to the identification of IL-4 and IL-10 as potential factors associated with pathogenicity. Further in vitro analysis showed that IL-4, but not IL-10, promoted IgG anti-Dsg3 Ab production by primed B cells. Additionally, adenoviral expression of soluble IL-4Rα in vivo suppressed IgG anti-Dsg3 Ab production and the PV phenotype, indicating a pathogenic role of IL-4. This strategy is useful for evaluating the effector function of autoreactive T cells involved in the pathogenesis of various autoimmune diseases. *The Journal of Immunology,* **2008, 181: 1526–1535.**

Autoreactive T cells are thought to play a central role in the pathogenesis of various autoimmune diseases (1). A number of studies using patient samples and animal models have identified and characterized the autoreactive T cells that potentially exert the pathogenic effector function. Recent reports using autoreactive T cell clones generated from patient samples indicate that a subset of autoreactive T cells has a pathogenic effector function in vitro (2). However, it has been difficult to evaluate whether the individual autoreactive T cells analyzed in vitro are actually involved in the autoimmune pathogenic process of patients in vivo. Autoreactive T cell clones have been shown to induce tissue damage in a mouse model for multiple sclerosis and insulin-dependent diabetes mellitus (3, 4), but the in vivo helper activity of autoreactive T cells has never been analyzed at a clonal level in mouse models for autoantibody-mediated autoimmune diseases.

Pemphigus vulgaris (PV)[3] is a life-threatening blistering disease involving IgG autoantibodies directed against desmoglein 3 (Dsg3). Dsg3 is a cadherin-type glycoprotein expressed on stratified squamous epithelium, including the skin and oral mucosa, and plays a critical role in cell-cell adhesion (5). Anti-Dsg3 autoantibodies bind to keratinocyte cell surfaces and induce cell detachment, resulting in blisters and erosions in the skin and mucous membranes as well as characteristic histological findings, such as suprabasilar acantholysis (6, 7). Dsg3-reactive CD4$^+$ T cells have been detected and characterized in PV patients and healthy individuals, but it remains unclear whether these autoreactive T cells can induce the PV phenotype in vivo. In this study, we developed a novel experimental system that evaluates the in vivo pathogenicity of individual Dsg3-reactive T cell clones. In this system, Dsg3-reactive T cell lines generated in vitro from Dsg3$^{-/-}$ mice were adoptively transferred into recipient immunodeficient Rag-2$^{-/-}$ mice (Dsg3$^{+/+}$) to examine whether T cell lines have the ability to induce the PV phenotype after adoptive transfer. Using this system, we identified IL-4 as a critical T cell-derived factor involved in the pathogenesis of PV.

Materials and Methods

Mice

Dsg3$^{-/-}$ mice with a mixed genetic background of 129/SV (H-2^b) and C57BL/6J (H-2^b) were obtained by mating male and female Dsg3$^{-/-}$ mice (The Jackson Laboratory) (8). C57BL/6 mice and C57BL/6 Rag-2$^{-/-}$ mice were purchased from the Central Institute for Experimental Animals (Tokyo, Japan). OT-II (OVA-specific) TCR transgenic mice (H-2^b) were originally generated by Barnden et al. (9), and Rag-2$^{-/-}$ OT-II transgenic mice (H-2^b) were kindly provided by Prof. S. Koyasu (Keio University). The Keio University Ethics Committee for Animal Experiments approved all experiments in this study.

Antigens

A baculoprotein rDsg3EHis, which includes the extracellular domain of mouse Dsg3 (amino acid residues 1–565), an E-tag, and a His-tag, was produced as described previously (10) with some modifications. In brief, the purification was improved by serial procedures using Talon affinity metal resin (Clontech Laboratories) followed by a HiTrap anti-E Tag column (GE Healthcare). Five mouse Dsg3 fragments (rDsg3-1–5) expressed in *Escherichia coli* were prepared as soluble maltose-binding protein (MalBP)-Dsg3 fusion proteins as described (11). The Dsg3 fragments encompassing together the entire 565-aa sequence of the extracellular domain of mouse Dsg3 included rDsg3-1 (aa 1–119), rDsg3-2 (aa 99–230),

*Department of Dermatology, †Institute for Advanced Medical Research, and ‡Division of Rheumatology, Department of Internal Medicine, Keio University School of Medicine, Tokyo, Japan

Received for publication January 30, 2008. Accepted for publication May 13, 2008.

The costs of publication of this article were defrayed in part by the payment of page charges. This article must therefore be hereby marked *advertisement* in accordance with 18 U.S.C. Section 1734 solely to indicate this fact.

[1] This work was supported by Grants-in-Aid for Scientific Research from the Ministry of Education, Culture, Sports, Science and Technology of Japan, the Health and Labour Sciences Research Grants for Research on Measures for Intractable Diseases from Ministry of Health, Labor and Welfare of Japan, and Keio Gakuji Academic Development Funds.

[2] Address correspondence and reprint requests to Dr. Masataka Kuwana, Division of Rheumatology, Department of Internal Medicine, Keio University School of Medicine, 35 Shinanomachi, Shinjuku-ku, Tokyo 160-8582, Japan. E-mail address: kuwanam@sc.itc.keio.ac.jp

[3] Abbreviations used in this paper: Dsg3, desmoglein 3; PV, pemphigus vulgaris; MalBP, maltose-binding protein.

Table I. *Primer sequences, optical annealing temperatures, and amplified sizes of genes analyzed in PCR*

Genes	Primers (5' to 3')	Annealing Temp. (°C)	Sizes (bp)
IL-2			
Sense	TGATGGACCTACAGGAGCTCCTGAG	60	168
Antisense	GAGTCAAATCCAGAACATGCCGCAG		
IL-4			
Sense	CGAAGAACACCACAGAGAGTGAGCT	60	181
Antisense	GACTCATTCATGGTGCAGCTTATCG		
IL-6			
Sense	CTGGTGACAACCACGGCCTCCCCT	60	601
Antisense	ATGCTTAGGCATAACGCACTAGGT		
IL-10			
Sense	TGAAGCTTCTATTCTAAGGCTGGCC	60	178
Antisense	CTGAGCTGCTGCAGGAATGATCATC		
IL-17			
Sense	GGTCAACCTCAAAGTCTTTAACTC	51	396
Antisense	AAATACAAGTAAGTTTGCTGAGAAACG		
IFN-γ			
Sense	GCTACACACTGCATCTTGGCTTTGC	60	939
Antisense	CCTGTTACTACCTGACACATTCGAG		
TGF-β			
Sense	GCTCACTGCTCTTGTGACAGCAAAG	60	362
Antisense	CAAGGACCTTGCTGTACTGTGTGTC		
CCR4			
Sense	GACTGTCCTCAGGATCACTTTCAGA	60	255
Antisense	CCCAACAAGAAGACCAAGGAGTAG		
CCR7			
Sense	AACCAAAAGCACAGCCTTCCTGT	60	299
Antisense	TGTACGTCAGTATCACCAGCCC		
CXCR3			
Sense	AAAGGCAGAGAAGCAGGCA	60	1275
Antisense	TTCAGGCTGAAATCCTGTGG		
CXCR5			
Sense	ATGGATGACCTGTACAAGGAACTG	60	282
Antisense	TGCAAAAGGCAGGATGAAGAC		
CRTH2			
Sense	GACAACTGCTCTCTAGGAGGAACT	60	1263
Antisense	ACCACAAACAGGATGAGTCCGT		
β-actin			
Sense	TGGAATCCTGTGGCATCCATGAAAC	60	227
Antisense	TAAAACGCAGCTCAGTAACAGTCCG		

rDsg3-3 (aa 210–345), rDsg3-4 (aa 325–455), and rDsg3-5 (aa 428–565). These recombinant proteins were dialyzed against PBS containing 0.5 mM $CaCl_2$, filter-sterilized, and stored at −80°C until use. The expression of recombinant Dsg3 fragments was evaluated by SDS-PAGE followed by Coomassie blue staining or immunoblotting probed with an anti-mouse Dsg3 mAb (AK7 or AK18) (7).

Recombinant adenovirus harboring Dsg3 and soluble cytokine receptors

Adenoviral vectors harboring the entire extracellular domain and transmembrane region of mouse Dsg3 (rDsg3ΔIC; aa 1–590) or the extracellular domain of cytokine receptors (IL-4Rα, IL-10Rα, and IFN-γR1) were constructed using the AdEasy adenoviral vector system (Stratagene) according to the manufacturer's instructions. rDsg3ΔIC was adenovirally expressed in COS cells, which were subjected to sonication in PBS containing 0.5 mM $CaCl_2$ and 0.01% Triton X-100. The cellular lysates were filter-sterilized and used in T cell cultures as a source of Dsg3. The expression of Dsg3 was evaluated by SDS-PAGE followed by immunoblotting with anti-mouse Dsg3 mAb and rabbit anti-actin polyclonal Ab (Sigma-Aldrich). For soluble cytokine receptors, the cDNA for the entire extracellular domain of each cytokine receptor was cloned from a spleen cDNA library and used to construct recombinant adenoviruses. Each recombinant adenovirus harboring a soluble cytokine receptor was concentrated by $CsCl_2$ density gradient centrifugation, dialyzed against PBS, and stocked at −80°C until use. The in vivo expression of soluble cytokine receptors was confirmed by immunoblotting plasma obtained from adenovirus-infected mice with goat anti-IL-4Rα, anti-IL-10Rα, or anti-IFN-γR1 polyclonal Abs (R&D Systems).

Ag-specific T cell lines

Footpads of $Dsg3^{-/-}$ mice were immunized with 5 μg of rDsg3EHis emulsified with CFA (Sigma-Aldrich). After 7 days, a single-cell suspension (3×10^6/well) was prepared from the popliteal lymph nodes and cultured in 24-well plates with a mixture of rDsg3-1–5 (5 μg/ml each) in complete medium (RPMI 1640, 2 mM L-glutamine, 1 mM pyruvate, 50 U/ml penicillin, and 50 μg/ml streptomycin) supplemented with 1% C57BL/6 mouse serum. The cells were stimulated twice with the mixture of rDsg3-1–5 in the presence of 10^6 autologous 40 Gy-irradiated splenocytes in complete medium containing 10% FBS (Cambrex). T-STIM without Con A (BD Biosciences) was added to a final concentration of 1% twice a week as a source of growth factors. T cell blasts were subsequently subjected to limiting dilution using round-bottom 96-well plates in the presence of irradiated autologous splenocytes (2×10^4/well), antigenic Dsg3 fragments, and 1% T-STIM without Con A.

T cell proliferation assay

Dsg3-specific T cell proliferation was measured by [^{3}H]thymidine uptake as described (11). In some experiments, bone marrow-derived dendritic cells, which were prepared by culturing C57BL/6 bone marrow cells with 10 ng/ml GM-CSF (PeproTech) for 7 days, were used as APCs. Before the coculture with T cells, the bone marrow-derived dendritic cells were pulsed with pAd-rDsg3ΔIC or mock vector-transduced COS cell lysates (100 μg/ml) and maturated with 10 μg/ml LPS (Sigma-Aldrich) for 24 h. MHC class II restriction was determined by evaluating the inhibitory effect on Ag-induced T cell proliferation of 4 μg/ml rat anti-I-A^b mAb (clone M5/114; BD Biosciences). An isotype-matched rat mAb to an irrelevant Ag (BD Biosciences) was used as a control.

Passive transfer

To evaluate the pathogenicity of Dsg3-reactive T cell lines, Dsg3-reactive T cell lines (10^6) and splenic $Dsg3^{-/-}$ B cells (5×10^6) were transferred into $Rag\text{-}2^{-/-}$ mice via the tail vein. In vivo-primed $Dsg3^{-/-}$ B cells were prepared by depleting $CD4^+$ and $CD8^+$ cells from the splenocytes of rDsg3EHis-immunized $Dsg3^{-/-}$ mice (10), followed by the positive selection of $B220^+$

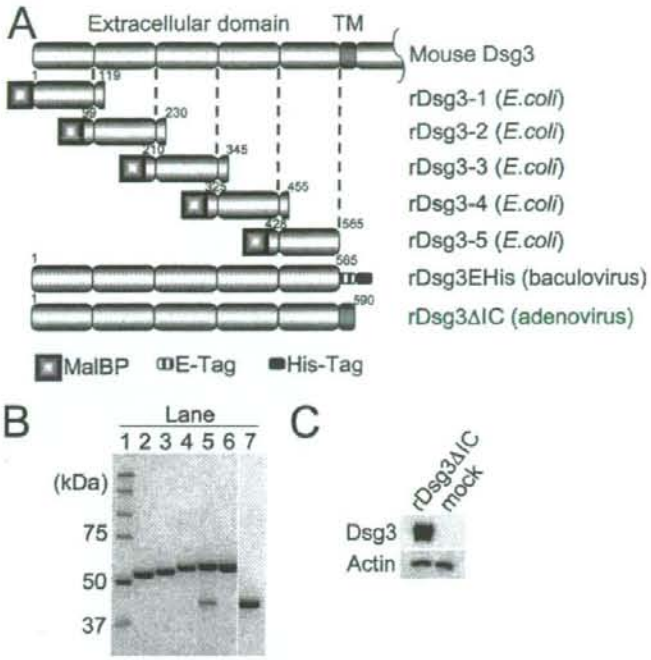

FIGURE 1. Recombinant mouse Dsg3 proteins. *A*, Schematic illustration of the mouse Dsg3 and recombinant Dsg3 proteins used in this study. rDsg3-1–5 are bacterial recombinant Dsg3 fragments fused to MalBP. rDsg3EHis is a baculovirally produced Dsg3 extracellular domain with an E-tag and His-tag at the carboxyl terminus. rDsg3ΔIC is adenovirally produced Dsg3 lacking the intracellular domain. The numbers indicate the positions of amino acid residues in Dsg3. TM, transmembrane domain. *B*, rDsg3-1–5 and MalBP visualized by Coomassie blue staining. *Lane 1*, molecular mass markers; *lanes 2–6*, rDsg3-1–5; *lane 7*, MalBP (*lane 7* is a different part of the same gel). *C*, Immunoblots of lysates from cells infected with the rDsg3ΔIC-harboring adenovirus vector or mock virus. Fractionated proteins were probed with anti-mouse Dsg3 or anti-actin Ab.

cells using the MACS cell separation system (Miltenyi Biotec). A portion of the separated $CD4^+$ and $CD8^+$ cells was used as unfractionated $Dsg3^{-/-}$ T cells. In some experiments, recombinant adenovirus harboring sIL-4Rα, sIL-10Rα, or sIFN-γR1 (10^9 infections units) was directly injected into Rag-$2^{-/-}$ mice via tail vein 5 days before the passive transfer of pathogenic Dsg3-reactive T cell clones and $Dsg3^{-/-}$-primed B cells. It has been demonstrated that recombinant adenovirus injected from tail vein mainly infects hepatocytes, resulting in expression of recombinant protein (12).

RT-PCR

T cell lines were stimulated with 25 ng/ml PMA (Sigma-Aldrich) and 1 μg/ml ionomycin (Sigma-Aldrich) for 3 days, and isolated using anti-CD4 mAb-coupled magnetic beads (Dynal Biotech). Total RNA was isolated from individual T cell lines using the RNeasy mini kit with RNase-free DNase (Qiagen). For the analysis of TCR Vβ gene usage, aliquots of the synthesized cDNA (5 ng of total RNA equivalent) were amplified using a

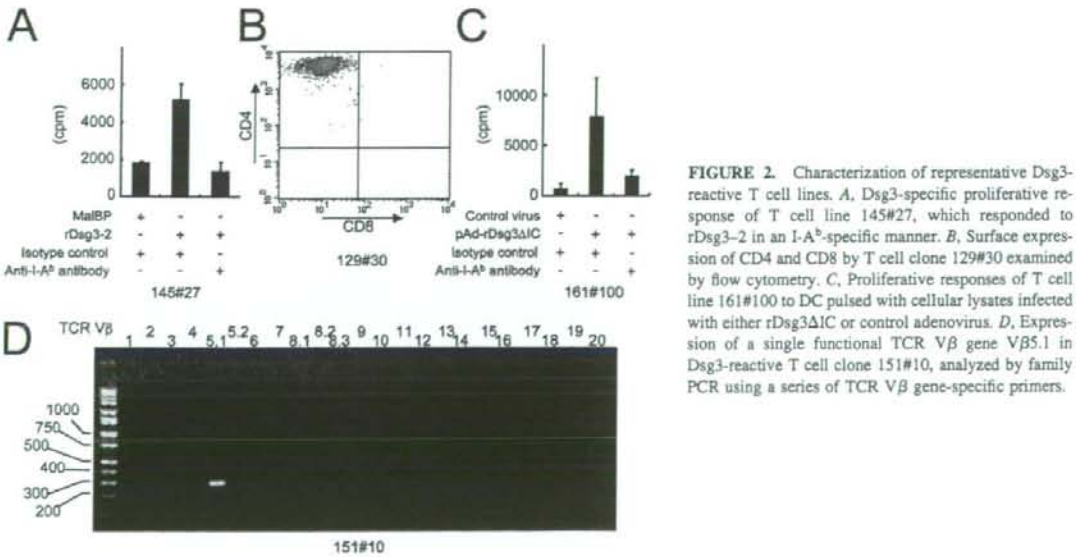

FIGURE 2. Characterization of representative Dsg3-reactive T cell lines. *A*, Dsg3-specific proliferative response of T cell line 145#27, which responded to rDsg3–2 in an I-A^b-specific manner. *B*, Surface expression of CD4 and CD8 by T cell clone 129#30 examined by flow cytometry. *C*, Proliferative responses of T cell line 161#100 to DC pulsed with cellular lysates infected with either rDsg3ΔIC or control adenovirus. *D*, Expression of a single functional TCR Vβ gene Vβ5.1 in Dsg3-reactive T cell clone 151#10, analyzed by family PCR using a series of TCR Vβ gene-specific primers.

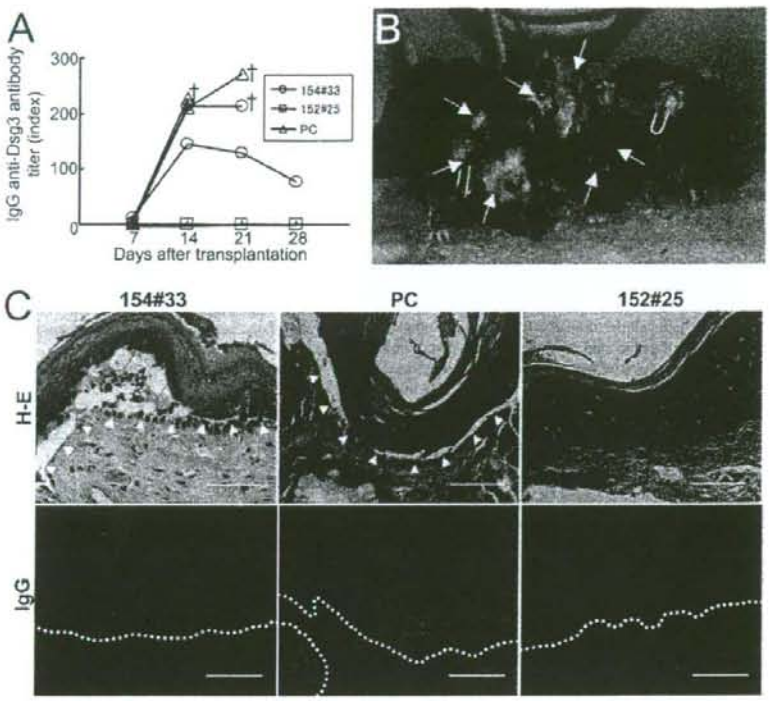

FIGURE 3. Evaluation of the in vivo pathogenicity of Dsg3-reactive T cell clones. *A*, Serial changes in the levels of IgG anti-Dsg3 Abs in mice that had been treated with the adoptive transfer of the Dsg3-reactive T cell clone 152#25 (□) or 154#33 (○). Mice were treated with $Dsg3^{-/-}$ unfractionated T cells as a positive control (PC, △). *B*, Skin phenotype of mice treated with 154#33 (*left*), $Dsg3^{-/-}$ T cells (*center*), or 152#25 (*right*) on day 22. Erosions and hair loss (arrows) were apparent in the periorbital area, nose, head, ears, and shoulders of mice treated with 154#33 or $Dsg3^{-/-}$ T cells. *C*, Histology (*upper panels*) and IgG deposition (*lower panels*) in the palate from recipient mice. Acantholytic blister (arrowheads) and IgG deposition on keratinocyte cell surfaces were observed in the 154#33-treated mouse, as observed in the $Dsg3^{-/-}$ T cell-treated mouse. Dotted lines indicate the basement membrane. Bars: 50 μm.

panel of TCR Vβ region-specific primers in combination with a Cβ region primer for 37 cycles. Primers for Vβ1–20 and Cβ were designed based on previous reports (13–15). The expression of cytokines and chemokine receptors was also examined by PCR using the specific primers listed in Table I for 38 and 40 cycles, respectively.

Flow cytometry

Surface markers of the Dsg3-reactive T cell lines were analyzed using FITC-conjugated anti-mouse CD4 mAb (clone GK1.5), FITC-conjugated anti-mouse CD8 mAb (clone 53-6.7), PE-conjugated anti-mouse TCRβ

Table II. *Characteristics of Dsg3-reactive T cell lines according to their in vivo pathogenicity*

Line Name	Antigenic Fragments	Functional TCR Vβ Gene Usage (Vβ)	Cytokine Expression							Chemokine Receptor Expression					In Vivo Production of Anti-Dsg3 Antibody
			IL-2	IL-4	IL-6	IL-10	IL-17	IFN-γ	TGF-β	CCR7	CCR4	CXCR5	CRTH2	CXCR3	
T cell lines with in vivo pathogenicity[a]															
140#27[b]	rDsg3-3	6	+	+	−	+	+	+	+	−	+	−	−	+	+
147#27[b]	rDsg3-3	8.2	+	+	+	+	−	+	+	+	+	+	−	+	+
147#48[b]	rDsg3-3	8.2	+	+	+	+	−	+	+	+	+	−	−	+	+
153#5	rDsg3-1	5, 7, 8.1	+	+	−	+	−	+	+	+	+	−	−	+	+
154#33[b]	rDsg3-1	8.2	+	+	+	+	+	+	+	+	+	+	−	+	+
161#100	rDsg3-1	6, 11	+	+	−	+	−	+	+	+	+	+	−	+	+
164#2[b]	rDsg3-3	6	+	+	−	+	−	+	+	+	+	−	−	+	+
T cell lines without in vivo pathogenicity[a]															
129#30[b]	rDsg3-3	8.3	+	−	−	−	−	+	+	+	+	−	−	+	−
141#70[b]	rDsg3-1	6	+	−	−	−	−	+	+	+	−	+	−	+	−
145#27	rDsg3−2, 4	6, 14	+	−	−	−	−	+	−	−	−	−	−	−	−
145#28	rDsg3-1	8.2, 11	+	+	+	+	−	+	+	−	−	−	−	+	−
146#13	rDsg3-2	1, 4	+	+	+	+	+	+	+	+	+	+	−	+	−
146#25	rDsg3-4	8.1, 15	+	−	−	+	−	+	−	−	−	+	−	−	−
151#10[b]	rDsg3-1	5.1	−	−	−	−	−	+	+	+	−	+	−	+	−
152#25[b]	rDsg3-1	1	−	+	−	−	−	+	+	+	+	−	−	+	−
159#11	rDsg3-1	3, 4	+	−	−	−	−	+	+	+	+	+	−	+	−
161#28[b]	rDsg3-2	6	+	+	−	+	+	+	+	+	+	+	−	+	−
161#29[b]	rDsg3-2	4	−	+	+	+	+	+	+	+	+	+	−	+	−
162#24[b]	rDsg3-1	8.1	+	−	−	−	+	+	+	+	+	+	+	+	−
162#92[b]	rDsg3-2	8.2	+	+	+	+	−	+	+	+	+	+	−	+	−

[a] Identification of in vivo pathogenicity requres anti-Dsg3 Ab production, IgG deposition on the epithelial cell surfaces of the palate, and acantholysis.
[b] Clonality was confirmed by TCR β-chain analysis.

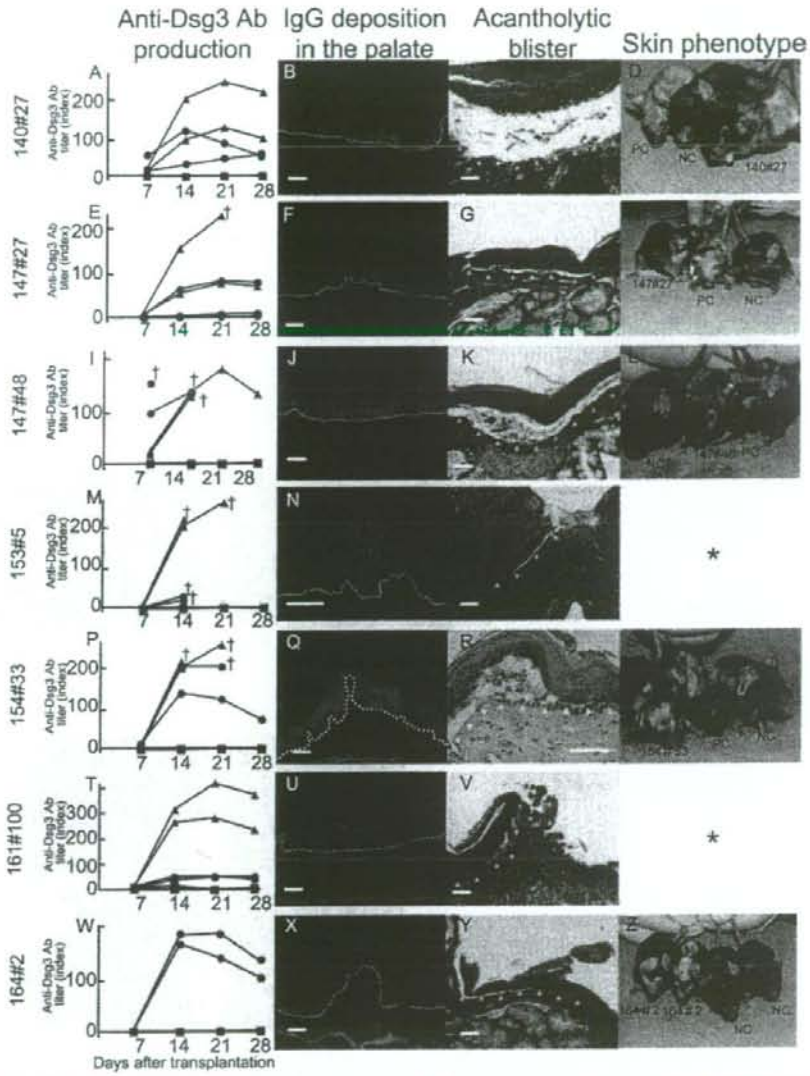

FIGURE 4. Anti-Dsg3 Ab production, IgG deposition in the palate, acantholytic blisters, and skin phenotype induced by individual Dsg3-reactive T cell lines with in vivo pathogenicity. 140#27, 147#27, 147#48, 154#33, and 164#2 were confirmed to be clones. *A*, *E*, *I*, *M*, *P*, *T*, and *W*, In the anti-Dsg3 Ab ELISA, the blue lines indicate mice with the transplanted T cell lines of interest, black lines indicate the positive control mice with transplanted Dsg3$^{-/-}$ T cells, and red lines indicate the negative control mice with transplanted B cells alone (*A* and *E*) or B cells in combination with a nonpathogenic clone 161#28 (*I*), 152#25 (*M*, *P*, and *T*), or 161#29 (*W*). Crosses indicate death. *B*, *F*, *J*, *N*, *Q*, *U*, and *X*, IgG deposition (green) in the palate was detected by immunostaining with an AlexaFluor 488-conjugated anti-mouse IgG Ab. Dotted lines indicate basement membrane. *C*, *G*, *K*, *O*, *R*, *V*, and *Y*, Acantholytic blisters (arrowheads) in the palate were evaluated by H&E staining. *D*, *H*, *L*, *S*, and *Z*, PC denotes the positive control mouse, and NC denotes the negative control mouse. Bars: 50 μm. Asterisks indicate that images are unavailable.

mAb (clone H57-597), and Cy-Chrome-conjugated anti-mouse CD4 mAb (clone H129.19), all of which were purchased from BD Biosciences. In some experiments, T cell lines labeled with 1 μM CFSE (Molecular Probes) were analyzed by flow cytometry after gating on the CD4$^+$TCRβ$^+$ population of the lymphocyte fraction.

Anti-Dsg3 Ab

IgG anti-Dsg3 Abs in plasma samples or culture supernatants were quantitatively measured using an ELISA as described previously (10). To examine the capacity of B cells to produce anti-Dsg3 Abs in vitro, MACS-sorted Dsg3$^{-/-}$ B cells were cultured with 500 ng/ml soluble CD40L (R&D Systems) in the presence of various concentrations of IL-4, IL-10, or IFN-γ (R&D Systems) for 7 days.

Histopathology

Formalin-fixed palate tissue was stained with H&E and observed with an inverted microscope TE2000-U (Nikon).

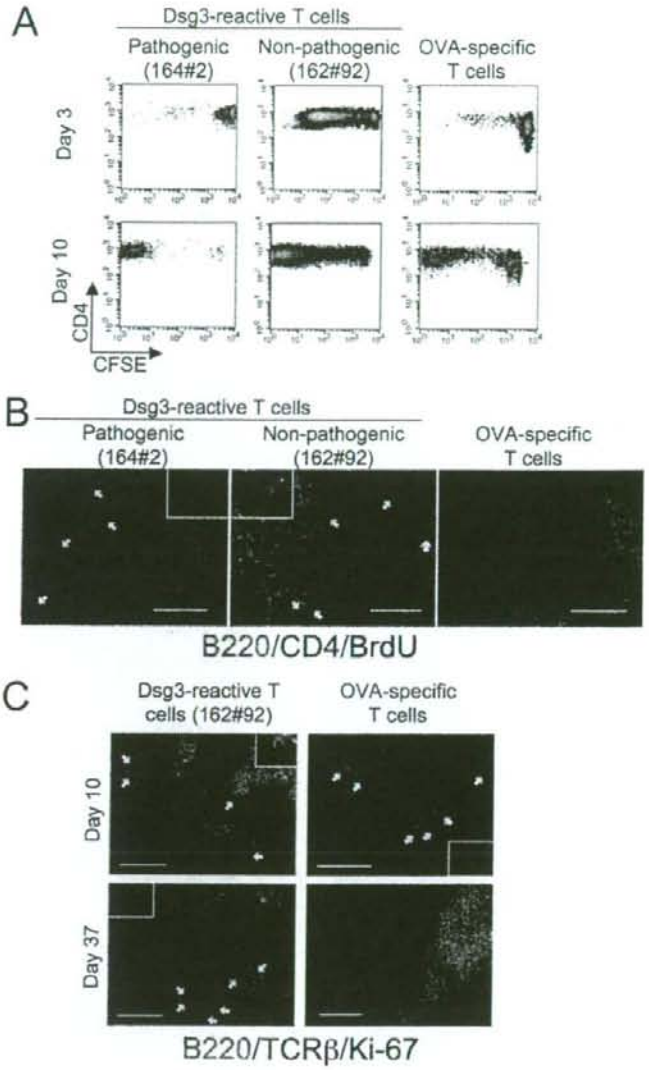

FIGURE 5. In vivo proliferative capacity of Dsg3-reactive T cell clones. *A*, Flow cytometric analysis of CFSE dilution in splenic $CD4^+TCR\beta^+$ T cells. After Dsg3-reactive T cell clone 164#2 (pathogenic), clone 162#92 (nonpathogenic), or OVA-specific T cells were labeled with CFSE in vitro, the T cells were transferred with $Dsg3^{-/-}$ B cells isolated from a Dsg3-immunized $Dsg3^{-/-}$ mouse into $Rag2^{-/-}$ mice. T cells were analyzed for CFSE dilution by flow cytometry after gating on the $CD4^+TCR\beta^+$ population of the splenocytes 3 and 10 days after transfer. *B*, Immunostaining for B220 (green), CD4 (blue), and BrdU (red) in the spleen from recipient mice 37 days after the transfer of Dsg3-reactive T cell clone 164#2 (pathogenic), clone 162#92 (nonpathogenic), or OVA-specific T cells. BrdU-bearing $CD4^+$ T cells (arrows) were detected in the region close to the B cell area in mice with transplanted Dsg3-reactive T cell lines. *C*, Immunostaining for B220 (green), TCRβ (blue), and Ki-67 (red) in the spleen from recipient mice on days 10 and 37 after the transfer of Dsg3-reactive T cell clone 162#92 or OVA-specific T cells. On day 37, Ki-67-positive T cells (arrows) were detected in mice with transplanted Dsg3-reactive T cell lines, but not in mice with transplanted OVA-specific T cells. Bars: 50 μm. Insets denote high-power views of T cells positive for BrdU or Ki-67.

Immunohistochemistry

For direct immunofluorescent staining, 10-μm cryosections of the palate were directly stained with AlexaFluor 488-conjugated anti-mouse IgG Abs (Molecular Probes) and observed using a fluorescence microscope (Nikon) to detect IgG deposits. For indirect staining, 6-μm cryosections of the spleen were fixed with acetone and subsequently stained with the appropriate combination of the following Abs: FITC-conjugated anti-mouse CD19 (clone 1D3), PE-conjugated anti-mouse TCRβ (clone H57-597), AlexaFluor 488-conjugated anti-mouse B220 (clone RA3-6B2), biotinylated anti-mouse CD4 (clone RM4-5, BD Biosciences), and anti-Ki-67 mAb (clone TEC-3; DakoCytomation). Secondary Abs included AlexaFluor 488-conjugated anti-mouse IgG, AlexaFluor 660-conjugated anti-rat IgG, and AlexaFluor 488-conjugated anti-FITC Abs, and AlexaFluor 568-conjugated streptavidin (Molecular Probes). BrdU staining was performed using AlexaFluor 660-conjugated anti-BrdU mAb (clone PRB-1, Molecular Probes), as previously described (16). Sections were observed under a confocal laser fluorescence microscope FV1000 (Olympus).

Statistical analysis

All continuous data are shown as the means ± SD. Two-tailed repeated-measures ANOVA, Fisher's exact probability test, or the Mann-Whitney *U* test was used as appropriate.

Results

Preparation of recombinant Dsg3 proteins

We prepared recombinant mouse Dsg3 fragments using three different expression systems (Fig. 1A). rDsg3EHis (10), a baculoprotein containing the entire extracellular domain of Dsg3, was used to immunize $Dsg3^{-/-}$ mice. rDsg3-1–5, a series of recombinant MalBP-Dsg3 fusion proteins produced in *E. coli*, were used to expand Dsg3-reactive T cells and to evaluate antigenic regions in vitro. The purity of each recombinant protein was >95% (Fig. 1*B*).

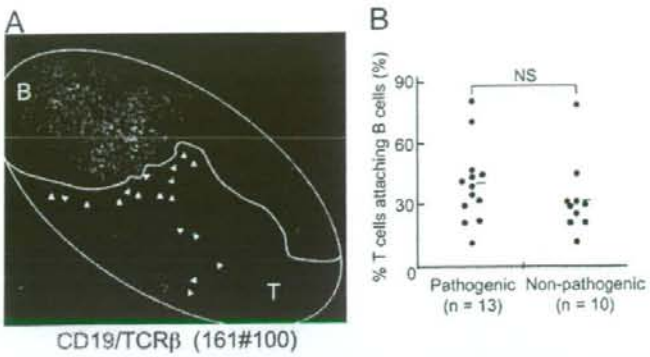

FIGURE 6. In vivo homing of transferred Dsg3-reactive T cell lines in the spleen. *A*, A representative image of CD19 (green) and TCRβ (red) in the spleen of mice with transplanted Dsg3-reactive T cell line 161#100. Based on the distribution of CD19 and TCRβ staining, the Dsg3-reactive T cells were classified into T cells within the B cell area (pink arrowheads) and those residing outside the B cell area (yellow arrowheads). The T cell area (T) and B cell area (B) are indicated with white outlines. *B*, The proportion of T cells within the B cell area of the total T cells in the spleen from mice with transplanted Dsg3-reactive T cell lines, according to the presence or absence of in vivo pathogenicity. A total of 165 lymphoid follicle-like structures were analyzed. Values were averaged in 23 individual mice and compared between the pathogenic (147#48, 153#5, 161#100, and 164#2) and nonpathogenic T cell lines (146#13, 152#25, 159#11, 161#28, and 162#24). Statistical analysis was performed by the Mann-Whitney *U* test. Horizontal bars indicate the mean.

Lysates from COS cells infected with pAd-rDsg3ΔIC, an adenovirus vector harboring Dsg3 cDNA lacking the sequence for the intracellular domain, were used to evaluate T cell reactivity to native Dsg3 produced in mammalian cells (Fig. 1*C*). Serial use of more than one Dsg3 preparation for T cell stimulation is useful to eliminate expansion of T cells responsive to contaminant proteins unique to individual Ag preparations.

Establishment of Dsg3-reactive T cell lines

To establish Dsg3-reactive T cell lines, the footpads of Dsg3$^{-/-}$ mice were immunized with rDsg3EHis emulsified with CFA. Single-cell suspensions of lymphocytes were prepared from the popliteal lymph nodes and were subsequently stimulated twice with a mixture of rDsg3-1–5 in vitro. The expanded cells that showed a specific proliferative response to at least one of the Dsg3 fragments were subjected to limiting dilution. From this selection, we obtained 59 T cell lines that were specifically reactive with one of rDsg3-1–4. All of these T cell lines were restricted by MHC class II (Fig. 2*A*) and expressed the CD4 surface marker (Fig. 2*B*). To evaluate whether these T cell lines responded to peptides generated from native Dsg3 through Ag processing, randomly selected T cell lines were cultured with bone marrow-derived dendritic cells pulsed with pAd-rDsg3ΔIC-infected and control adenovirus-infected cell lysates. All the T cell lines examined showed a specific response to Dsg3-expressing cell lysates in a MHC class II-dependent manner (Fig. 2*C*). The in vitro-generated T cell lines were reactive to two different Dsg3 preparations, indicating that they were specific for Dsg3. Eighteen Dsg3-reactive T cell lines were confirmed to be clones based on their expression of a single functional TCR Vβ-chain, determined by family PCR combined with a direct nucleotide sequencing (Fig. 2*D*).

In vivo pathogenicity of Dsg3-reactive T cell lines

Twenty Dsg3-reactive T cell lines, including 13 clones expressing single functional TCR Vβ-chain, were further evaluated for their in vivo pathogenicity. Since our previous study demonstrated that splenic T cells and B cells are required to induce experimental PV (17), the individual T cell lines were transferred into Rag-2$^{-/-}$ mice together with primed B cells isolated from the spleen of a rDsg3EHis-immunized Dsg3$^{-/-}$ mouse. In a representative experiment, clone 154#33 effectively promoted the production of IgG anti-Dsg3 Abs in vivo (Fig. 3*A*) and subsequently induced a PV phenotype, consisting of skin erosions and hair loss (Fig. 3*B*). Mice into which clone 154#33 was transferred showed acantholytic blisters and in vivo IgG deposition on keratinocyte cell surfaces (Fig. 3*C*). These PV features were also observed in positive control mice, into which unfractionated Dsg3$^{-/-}$ T cells had been transferred instead of Dsg3-reactive T cell lines. In contrast, transplantation of another clone, 152#25, failed to induce the IgG anti-Dsg3 Ab production or the PV phenotype, indicating that only a subset of the Dsg3-reactive T cell lines possessed in vivo pathogenic activity. The PV phenotype was not observed in control mice that received primed Dsg3$^{-/-}$ B cells alone or in combination with irrelevant OVA-specific T cells derived from Rag-2$^{-/-}$ OT-II transgenic mice (data not shown).

As summarized in Table II, 7 of the Dsg3-reactive T cell lines, including 5 clones, induced the PV phenotype in vivo, and thus were regarded as pathogenic lines; in contrast, 13 of the Dsg3-reactive T cell lines failed to induce the PV phenotype. A total of 86 mice were used for this analysis. Results regarding the PV phenotype induction were completely reproducible: none of the nonpathogenic T cell lines induced the PV phenotype despite several attempts. Detailed data on the anti-Dsg3 Ab production, histological findings, and skin phenotype in mice receiving transplants of six additional Dsg3-reactive T cell lines possessing in vivo pathogenicity are shown in Fig. 4. Interestingly, the in vivo production of IgG anti-Dsg3 Abs and the PV skin phenotype in mice receiving Dsg3-reactive T cell lines were completely concordant, suggesting a direct pathogenic role of the anti-Dsg3 Ab response in our PV model.

In vivo behavior of Dsg3-reactive T cells

To analyze the fate of the transferred autoreactive T cells, we examined whether the transplanted Dsg3-reactive T cells proliferated in vivo in the recipient Rag-2$^{-/-}$ mice, using several different systems. First, Dsg3-reactive or OVA-specific T cells were labeled with CFSE and transferred into Rag-2$^{-/-}$ mice in combination with primed Dsg3$^{-/-}$ B cells. On the 10th day after adoptive transfer, diluted CFSE was detected in the spleen of mice treated with pathogenic and nonpathogenic Dsg3-reactive T cell lines as well as

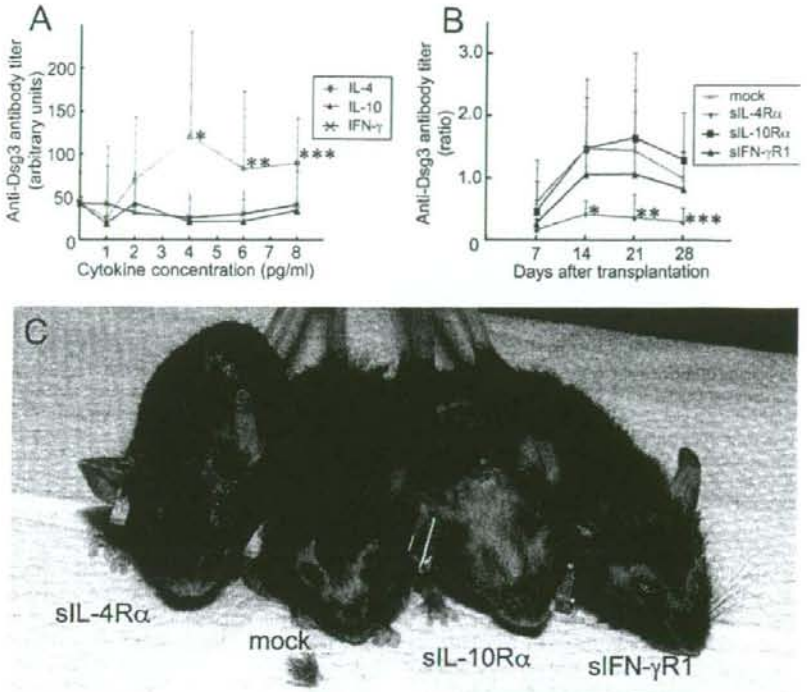

FIGURE 7. Role of T cell-derived cytokines in experimental PV. *A*, IgG anti-Dsg3 Ab titers in the culture supernatants of primed B cells. Splenic B cells from rDsg3EHis-immunized Dsg3$^{-/-}$ mice were cultured for 7 days with recombinant soluble CD40L in the presence of IL-4, IL-10, or IFN-γ at the concentrations indicated. Values shown are the means and SD of 16 individual experiments. Statistical analysis was performed by two-tail repeated measures ANOVA. *, $p = 0.0002$; **, $p = 0.008$; ***, $p = 0.01$. *B*, Effects of cytokine blockade on anti-Dsg3 Ab production in mice with transplanted Dsg3-reactive T cell clones. Serial IgG anti-Dsg3 Ab titers in plasma from mice expressing adenovirus-borne sIL-4Rα, sIL-10Rα, or sIFN-γR1 and subsequently undergoing adoptive transfer of pathogenic Dsg3-reactive T cell clone 147#48. Values are the mean and SD of six independent experiments, shown as a ratio to the Ab titer on day 28 in mock-treated mice. Statistical analysis was performed by two-tail repeated-measures ANOVA. *, $p = 0.03$; **, $p = 0.04$; ***, $p = 0.02$. *C*, Effects of cytokine blockade on the skin phenotype of mice 14 days after the adoptive transfer of pathogenic Dsg3-reactive T cell clone 147#48. Note the lack of erosion or hair loss in a mouse pretreated with adenovirus vector harboring sIL-4Rα.

those receiving irrelevant OVA-specific T cells (Fig. 5*A*), indicating that the transferred T cells were viable and expanded in vivo irrespective of their antigenic specificity or pathogenic activity. This early and nonspecific T cell proliferation was consistent with homeostatic proliferation (18, 19), which is a proliferative response of mature T cells in the lymphopenic environment to restore the lymphocyte pool size (20). Since it has been reported that the influence of homeostatic proliferation is negligible beyond 30 days of transfer (21), T cell proliferation was evaluated on day 37 by BrdU incorporation in the spleen of recipient mice. BrdU-bearing proliferating CD4$^+$ T cells were frequently detected in mice treated with Dsg3-reactive T cell lines irrespective of their pathogenicity, but not in mice treated with irrelevant OVA-specific T cells (Fig. 5*B*). The in vivo expansion of the Dsg3-reactive T cells was further evaluated by the expression of Ki-67, a marker for cell proliferation. In recipient mice, Dsg3-reactive and OVA-specific T cells expressed Ki-67 with similar frequencies on day 10, but Ki-67 expression was exclusively detected in the Dsg3-reactive T cells, irrespective of their pathogenicity, on day 37 (Fig. 5*C*). These findings together indicate that the transferred Dsg3-reactive T cells persistently proliferate in vivo, independent of their pathogenicity. Thus, the in vivo proliferative capacity did not account for the presence or absence of the in vivo pathogenicity of individual T cell lines.

Comparison of characteristics between Dsg3-reactive T cell lines with and without in vivo pathogenicity

Table II summarizes the antigenic Dsg3 fragments, functional TCR Vβ gene usage, and expression profiles of cytokines (IL-2, IL-4, IL-6, IL-10, IL-17, IFN-γ, and TGF-β) and chemokine receptors (CCR4, CCR7, CXCR3, CXCR5, and CRTH2) in the 20 Dsg3-reactive T cell lines evaluated for their pathogenicity, which included 13 clones. To identify T cell-derived factors associated with in vivo pathogenicity, the individual characteristics were compared between the 7 T cell lines with in vivo pathogenicity and the 13 lines without it. This analysis showed that all of the pathogenic T cell lines expressed IL-4 and IL-10, and the frequency of lines expressing IL-4 or IL-10 was significantly higher in the pathogenic than in the nonpathogenic group ($p = 0.045$ for both comparisons). There was no significant difference in the other characteristics between these two groups.

To examine the in vivo homing profiles of the transferred Dsg3-reactive T cell lines, spleen sections were stained with TCRβ for Dsg3-reactive T cells and with CD19 for B cells. Both the Dsg3-reactive T cell lines and the B cells had accumulated in the spleen and formed a lymphoid follicle-like structure. The Dsg3-reactive T cells were mainly detected in the T cell area, but some had infiltrated into the B cell area (Fig. 6*A*). There was no difference in the

number of T cells within the B cell area between mice treated with pathogenic T cell lines and those treated with nonpathogenic T cell lines (Fig. 6*B*), indicating that the presence or absence of pathogenicity in the Dsg3-reactive T cell lines was not due to a difference in the in vivo homing profiles.

A role of IL-4 in the pathogenesis of PV

We next assessed the roles of IL-4 and IL-10 released by Dsg3-reactive T cells in the mouse PV model, in vitro and in vivo. First, the IgG anti-Dsg3 Abs produced in vitro were measured in the culture supernatants of splenic B cells from rDsg3EHis-immunized Dsg3$^{-/-}$ mice stimulated with soluble recombinant CD40L in the presence of exogenous IL-4, IL-10, or IFN-γ. As shown in Fig. 7*A*, IL-4 significantly promoted the production of IgG anti-Dsg3 Abs from primed Dsg3$^{-/-}$ B cells, but neither IL-10 nor IFN-γ had such activity. Next, recombinant adenovirus harboring soluble cytokine receptors (IL-4Rα, IL-10Rα, or IFN-γR1) was administered to Rag-2$^{-/-}$ mice via the tail vein to neutralize IL-4, IL-10, or IFN-γ in vivo. Five days later, the pathogenic Dsg3-reactive T cell clone 147#48 and primed Dsg3$^{-/-}$ B cells were adoptively transferred into immunodeficient mice. The in vivo expression of soluble IL-4Rα significantly suppressed the IgG anti-Dsg3 Ab production (Fig. 7*B*) and the PV skin phenotype (Fig. 7*C*), but the expression of soluble IL-10Rα or soluble IFN-γR1 had no effect. Concordant results were obtained from six independent experiments using clone 147#48, and from four experiments using another pathogenic clone, 164#2.

Discussion

We successfully established a novel evaluation system for the in vivo pathogenicity of Ag-specific T cells at a clonal level, by performing the adoptive transfer of in vitro-generated Ag-specific T cell clones into immunodeficient Rag-2$^{-/-}$ mice in combination with in vivo-primed B cells. We confirmed that the transferred Dsg3-reactive T cells proliferated persistently and homed to the secondary lymphoid tissue in vivo, but only a subset of the T cell lines were able to induce the disease phenotype. Additionally, the capacity of Dsg3-reactive T cell lines to induce anti-Dsg3 Ab production was completely concordant with the PV phenotype expression, confirming previous reports showing that the anti-Dsg3 autoantibody has a direct role in inducing PV in human patients (6) and in a mouse model (7). More importantly, this study directly demonstrates that a single Ag-specific CD4$^+$ T cell is capable of inducing autoimmune disease phenotype through pathogenic autoantibody production. Finally, the classification of Dsg3-reactive T cell lines into pathogenic and nonpathogenic lines enabled us to identify T cell-derived IL-4 as a critical molecule driving PV in the mouse model. Our experimental system is applicable to other autoimmune diseases in which the autoimmune targets are identified, and it is useful not only for screening the in vivo pathogenicity of autoantigen-specific T cells, but also for identifying molecules and pathways critically involved in the pathogenic autoimmune process. The in vitro establishment of autoantigen-reactive T cell lines is the most time-consuming step in our procedure, but once specific T cell lines are available, their in vivo pathogenic activity and behavior can be readily evaluated.

Our in vivo finding that T cell-derived IL-4 plays a critical role in this mouse model of PV may also be relevant to human PV, because a previous report demonstrated the presence of Dsg3-reactive T cells capable of producing IL-4 in PV patients, but not in healthy controls (22). Since we showed that exogenous IL-4 directly stimulated B cells to produce anti-Dsg3 Abs in vitro, IL-4 produced by Dsg3-reactive T cells is likely to play an essential role in pathogenic anti-Dsg3 autoantibody production. Our results further indicate that IL-4 is essential but not enough to induce PV phenotype, because some of the nonpathogenic Dsg3-reactive T cell lines express IL-4. The pathogenic role of T cell-derived IL-4 has been previously investigated in mouse models for several autoantibody-mediated autoimmune diseases. For example, in experimental autoimmune myasthenia gravis, the disease phenotype is more severe and lasts longer in IL-4$^{-/-}$ mice, indicating a role for IL-4 in preventing the disease (23, 24). In this regard, it has been shown that acetylcholine receptor-reactive T cell clones generated from myasthenia gravis patients fail to secrete IL-4 (25), and that acetylcholine receptor-stimulated IL-4 secretion from PBMC is rarely detected in myasthenia gravis patients (26). Additionally, experimental Graves' disease can be induced in IFN-γ$^{-/-}$ mice, but not in IL-4$^{-/-}$ mice, indicating a requirement for IL-4 in disease induction (27), while IL-4 was shown to exert an inhibitory effect in another mouse model for Graves' disease (28). These inconsistent results suggest that the roles of IL-4 in the pathogenic processes of autoantibody-mediated autoimmune diseases are complex, but they may also reflect the limitation of studies using gene-deficient mice to evaluate the roles of cytokines in autoimmune pathogenesis. Congenital defects in systemic cytokine production are known to affect the physiologic development of the immune system. Moreover, IL-4 secreted by non-T cells could potentially regulate the autoimmune pathogenesis. Our system enables the in vivo effector function of autoreactive T cell clones to be evaluated without the influence of these factors.

It is unclear what determines the nature of Dsg3-reactive T cells in terms of pathogenicity. Our results clearly show that there were a wide variety of gene expression profiles among Dsg3-reacive T cell clones. This heterogeneity is probably generated in a hierarchy during T cell development, and Dsg3-reactive T cells with all of the quantitative and qualitative features required for the PV phenotype induction in our experimental system were regarded as pathogenic clones. Therefore, it is probable that nonpathogenic Dsg3-reactive T cell clones may be able to induce the PV phenotype when missing factors would be supplemented with an appropriate microenvironment. In this regard, it would be interesting to examine if transfer of a large number of the nonpathogenic T cell clone or transfer of the nonpathogenic T cell clone in the presence of exogenous IL-4 would induce the PV phenotype.

Although systemic corticosteroids and other immunosuppressants have been shown to reduce the mortality rate in PV patients, some cases are still refractory to these conventional therapies (29). Recent reports showing remarkable effects of biologics targeting molecules critically involved in the pathogenic process, such as TNF-α and IL-6, have resulted in dramatic changes in the treatment algorithms of several inflammatory diseases, including rheumatoid arthritis and Crohn's disease (30–32). Therefore, anti-IL-4 biologics are a potential therapeutic strategy for refractory PV. In this regard, humanized anti-IL-4 mAb and soluble IL-4Rα have already been manufactured for the treatment of allergic diseases, such as asthma, and shown to be well tolerated in clinical trials (33, 34). Further studies are necessary to evaluate the efficacy of anti-IL-4 biologics in patients with severe PV.

Acknowledgments

We are grateful to S. Koyasu (Keio University) for providing the Rag-2$^{-/-}$ OT-II transgenic mice, T. Randall and K. Kusser (Trudeau Institute) for advice on BrdU staining, S. Ito for mouse management, and M. Suzuki for the preparation of cryosections.

Disclosures

The authors have no financial conflicts of interest.

References

1. Janeway, C. A., Jr., P. Travers, M. Walport, and M. J. Shlomchik. 2005. Autoimmunity and transplantation. In *Immunobiology, the Immune System in Health and Disease*, 6th Ed. E. Lawrence, ed. Garland Science Publishing, New York, pp. 557–612.
2. Kuwana, M., T. A. Medsger, Jr., and T. M. Wright. 2000. Analysis of soluble and cell surface factors regulating anti-DNA topoisomerase I autoantibody production demonstrates synergy between Th1 and Th2 autoreactive T cells. *J. Immunol.* 164: 6138–6146.
3. Zamvil, S., P. Nelson, J. Trotter, D. Mitchell, R. Knobler, R. Fritz, and L. Steinman. 1985. T-cell clones specific for myelin basic protein induce chronic relapsing paralysis and demyelination. *Nature* 317: 355–358.
4. Utsugi, T., J. W. Yoon, B. J. Park, M. Imamura, N. Averill, S. Kawazu, and P. Santamaria. 1996. Major histocompatibility complex class I-restricted infiltration and destruction of pancreatic islets by NOD mouse-derived β-cell cytotoxic $CD8^+$ T-cell clones in vivo. *Diabetes* 45: 1121–1131.
5. Amagai, M., V. Klaus-Kovtun, and J. R. Stanley. 1991. Autoantibodies against a novel epithelial cadherin in pemphigus vulgaris, a disease of cell adhesion. *Cell* 67: 869–877.
6. Amagai, M., T. Hashimoto, N. Shimizu, and T. Nishikawa. 1994. Absorption of pathogenic autoantibodies by the extracellular domain of pemphigus vulgaris antigen (Dsg3) produced by baculovirus. *J. Clin. Invest.* 94: 59–67.
7. Tsunoda, K., T. Ota, M. Aoki, T. Yamada, T. Nagai, T. Nakagawa, S. Koyasu, T. Nishikawa, and M. Amagai. 2003. Induction of pemphigus phenotype by a mouse monoclonal antibody against the amino-terminal adhesive interface of desmoglein 3. *J. Immunol.* 170: 2170–2178.
8. Koch, P. J., M. G. Mahoney, H. Ishikawa, L. Pulkkinen, J. Uitto, L. Shultz, G. F. Murphy, D. Whitaker-Menezes, and J. R. Stanley. 1997. Targeted disruption of the pemphigus vulgaris antigen (desmoglein 3) gene in mice causes loss of keratinocyte cell adhesion with a phenotype similar to pemphigus vulgaris. *J. Cell Biol.* 137: 1091–1102.
9. Barnden, M. J., J. Allison, W. R. Heath, and F. R. Carbone. 1998. Defective TCR expression in transgenic mice constructed using cDNA-based α- and β-chain genes under the control of heterologous regulatory elements. *Immunol. Cell Biol.* 76: 34–40.
10. Amagai, M., K. Tsunoda, H. Suzuki, K. Nishifuji, S. Koyasu, and T. Nishikawa. 2000. Use of autoantigen-knockout mice in developing an active autoimmune disease model for pemphigus. *J. Clin. Invest.* 105: 625–631.
11. Kuwana, M., T. A. Medsger, Jr., and T. M. Wright. 1995. T cell proliferative response induced by DNA topoisomerase I in patients with systemic sclerosis and healthy donors. *J. Clin. Invest.* 96: 586–596.
12. Wood, M., P. Perrotte, E. Onishi, M. E. Harper, C. Dinney, L. Pagliaro, and D. R. Wilson. 1999. Biodistribution of an adenoviral vector carrying the luciferase reporter gene following intravesical or intravenous administration to a mouse. *Cancer Gene Ther.* 6: 367–372.
13. Casanova, J. L., P. Romero, C. Widmann, P. Kourilsky, and J. L. Maryanski. 1991. T cell receptor genes in a series of class I major histocompatibility complex-restricted cytotoxic T lymphocyte clones specific for a *Plasmodium berghei* nonapeptide: implications for T cell allelic exclusion and antigen-specific repertoire. *J. Exp. Med.* 174: 1371–1383.
14. Baker, F. J., M. Lee, Y. H. Chien, and M. M. Davis. 2002. Restricted islet-cell reactive T cell repertoire of early pancreatic islet infiltrates in NOD mice. *Proc. Natl. Acad. Sci. USA* 99: 9374–9379.
15. Friedman, T. M., M. Gilbert, C. Briggs, and R. Korngold. 1998. Repertoire analysis of $CD8^+$ T cell responses to minor histocompatibility antigens involved in graft-versus-host disease. *J. Immunol.* 161: 41–48.
16. Moyron-Quiroz, J. E., J. Rangel-Moreno, K. Kusser, L. Hartson, F. Sprague, S. Goodrich, D. L. Woodland, F. E. Lund, and T. D. Randall. 2004. Role of inducible bronchus associated lymphoid tissue (iBALT) in respiratory immunity. *Nat. Med.* 10: 927–934.
17. Tsunoda, K., T. Ota, H. Suzuki, M. Ohyama, T. Nagai, T. Nishikawa, M. Amagai, and S. Koyasu. 2002. Pathogenic autoantibody production requires loss of tolerance against desmoglein 3 in both T and B cells in experimental pemphigus vulgaris. *Eur. J. Immunol.* 32: 627–633.
18. Freitas, A. A., and B. B. Rocha. 1993. Lymphocyte lifespans: homeostasis, selection and competition. *Immunol. Today* 14: 25–29.
19. Bell, E. B., and S. M. Sparshott. 1997. The peripheral T-cell pool: regulation by non-antigen induced proliferation? *Semin. Immunol.* 9: 347–353.
20. Jameson, S. C. 2002. Maintaining the norm: T-cell homeostasis. *Nat. Rev. Immunol.* 2: 547–556.
21. Cannons, J. L., L. J. Yu, D. Jankovic, S. Crotty, R. Horai, M. Kirby, S. Anderson, A. W. Cheever, A. Sher, and P. L. Schwartzberg. 2006. SAP regulates T cell-mediated help for humoral immunity by a mechanism distinct from cytokine regulation. *J. Exp. Med.* 203: 1551–1565.
22. Veldman, C. M., K. L. Gebhard, W. Uter, R. Wassmuth, J. Grotzinger, E. Schultz, and M. Hertl. 2004. T cell recognition of desmoglein 3 peptides in patients with pemphigus vulgaris and healthy individuals. *J. Immunol.* 172: 3883–3892.
23. Balasa, B., C. Deng, J. Lee, P. Christadoss, and N. Sarvetnick. 1998. The Th2 cytokine IL-4 is not required for the progression of antibody-dependent autoimmune myasthenia gravis. *J. Immunol.* 161: 2856–2862.
24. Ostlie, N., M. Milani, W. Wang, D. Okita, and B. M. Conti-Fine. 2003. Absence of IL-4 facilitates the development of chronic autoimmune myasthenia gravis in C57BL/6 mice. *J. Immunol.* 170: 604–612.
25. Moiola, L., P. Karachunski, M. P. Protti, J. F. Howard, Jr., and B. M. Conti-Tronconi. 1994. Epitopes on the β subunit of human muscle acetylcholine receptor recognized by $CD4^+$ cells of myasthenia gravis patients and healthy subjects. *J. Clin. Invest.* 93: 1020–1028.
26. Yi, Q., R. Ahlberg, R. Pirskanen, and A. K. Lefvert. 1994. Acetylcholine receptor-reactive T cells in myasthenia gravis: evidence for the involvement of different subpopulations of T helper cells. *J. Neuroimmunol.* 50: 177–186.
27. Dogan, R. N., C. Vasu, M. J. Holterman, and B. S. Prabhakar. 2003. Absence of IL-4, and not suppression of the Th2 response, prevents development of experimental autoimmune Graves' disease. *J. Immunol.* 170: 2195–2204.
28. Nagayama, Y., H. Mizuguchi, T. Hayakawa, M. Niwa, S. M. McLachlan, and B. Rapoport. 2003. Prevention of autoantibody-mediated Graves'-like hyperthyroidism in mice with IL-4, a Th2 cytokine. *J. Immunol.* 170: 3522–3527.
29. Harman, K. E., S. Albert, and M. M. Black. 2003. Guidelines for the management of pemphigus vulgaris. *Br. J. Dermatol.* 149: 926–937.
30. Elliott, M. J., R. N. Maini, M. Feldmann, J. R. Kalden, C. Antoni, J. S. Smolen, B. Leeb, F. C. Breedveld, J. D. Macfarlane, H. Bijl, et al. 1994. Randomised double-blind comparison of chimeric monoclonal antibody to tumour necrosis factor alpha (cA2) versus placebo in rheumatoid arthritis. *Lancet* 344: 1105–1110.
31. Stack, W. A., S. D. Mann, A. J. Roy, P. Heath, M. Sopwith, J. Freeman, G. Holmes, R. Long, A. Forbes, and M. A. Kamm. 1997. Randomised controlled trial of CDP571 antibody to tumour necrosis factor-alpha in Crohn's disease. *Lancet* 349: 521–524.
32. Choy, E. H., D. A. Isenberg, T. Garrood, S. Farrow, Y. Ioannou, H. Bird, N. Cheung, B. Williams, B. Hazleman, R. Price, et al. 2002. Therapeutic benefit of blocking interleukin-6 activity with an anti-interleukin-6 receptor monoclonal antibody in rheumatoid arthritis: a randomized, double-blind, placebo-controlled, dose-escalation trial. *Arthritis Rheum.* 46: 3143–3150.
33. Hart, T. K., M. N. Blackburn, M. Brigham-Burke, K. Dede, N. Al-Mahdi, P. Zia-Amirhosseini, and R. M. Cook. 2002. Preclinical efficacy and safety of pascolizumab (SB 240683): a humanized anti-interleukin-4 antibody with therapeutic potential in asthma. *Clin. Exp. Immunol.* 130: 93–100.
34. Borish, L. C., H. S. Nelson, M. J. Lanz, L. Claussen, J. B. Whitmore, J. M. Agosti, and L. Garrison. 1999. Interleukin-4 receptor in moderate atopic asthma: a phase I/II randomized, placebo-controlled trial. *Am. J. Respir. Crit. Care Med.* 160: 1816–1823.

Helicobacter pylori eradication shifts monocyte Fcγ receptor balance toward inhibitory FcγRIIB in immune thrombocytopenic purpura patients

Atsuko Asahi,[1,2] Tetsuya Nishimoto,[1] Yuka Okazaki,[1] Hidekazu Suzuki,[3] Tatsuhiro Masaoka,[3] Yutaka Kawakami,[4] Yasuo Ikeda,[2] and Masataka Kuwana[1]

[1]Division of Rheumatology, [2]Division of Hematology, and [3]Division of Gastroenterology and Hepatology, Department of Internal Medicine, and [4]Institute for Advanced Medical Research, Keio University School of Medicine, Tokyo, Japan.

Immune thrombocytopenia purpura (ITP) is a bleeding disorder in which platelet-specific autoantibodies cause a loss of platelets. In a subset of patients with ITP and infected with *Helicobacter pylori*, the number of platelets recovers after eradication of *H. pylori*. To examine the role of *H. pylori* infection in the pathogenesis of ITP, the response of 34 ITP patients to treatment with a standard *H. pylori* eradication regimen, irrespective of whether they were infected with *H. pylori*, was evaluated. Eradication of *H. pylori* was achieved in all *H. pylori*–positive patients, and a significant increase in platelets was observed in 61% of these patients. By contrast, none of the *H. pylori*–negative patients showed increased platelets. At baseline, monocytes from the *H. pylori*–positive patients exhibited an enhanced phagocytic capacity and low levels of the inhibitory Fcγ receptor IIB (FcγRIIB). One week after starting the *H. pylori* eradication regimen, this activated monocyte phenotype was suppressed and improvements in autoimmune and platelet kinetic parameters followed. Modulation of monocyte FcγR balance was also found in association with *H. pylori* infection in individuals who did not have ITP and in mice. Our findings strongly suggest that the recovery in platelet numbers observed in ITP patients after *H. pylori* eradication is mediated through a change in FcγR balance toward the inhibitory FcγRIIB.

Introduction

Immune thrombocytopenia purpura (ITP) is an autoimmune disorder caused by increased platelet clearance by anti-platelet autoantibodies (1). In 1998, Gasbarrini et al. reported increase in platelet count in ITP patients infected with *Helicobacter pylori* after successful eradication of this bacterium (2). Recent accumulating evidence in Italy and Japan indicates that the eradication of *H. pylori* is effective in increasing the platelet count in nearly half of *H. pylori*–infected patients with idiopathic ITP (3, 4). In addition, a recent report showed that this platelet response lasts for years and cases of relapse are few (5). Based on its efficacy, good safety profile, and low cost, *H. pylori* eradication therapy for adult ITP is becoming very popular in several countries. Some investigators have suggested that the efficacy of *H. pylori* eradication in ITP patients may be mediated by *H. pylori*–independent mechanisms, such as immunomodulatory effects of the drugs used for the regimen (3), but we recently reported its complete lack of efficacy in *H. pylori*–uninfected ITP patients in a prospective study in which the patients were treated with a standard *H. pylori* eradication regimen irrespective of their *H. pylori* infection status (6). This finding clearly indicates that the platelet recovery observed in ITP patients after the eradication regimen results from the disappearance of *H. pylori* itself.

Several hypotheses have been proposed regarding the mechanism by which *H. pylori* might induce the development of ITP. One is that Abs to *H. pylori* components cross-react with platelet surface antigens. In this regard, Takahashi et al. reported that platelet eluates from *H. pylori*–positive ITP patients recognized the cytotoxin-associated gene A (CagA), one of the *H. pylori*–derived proteins that determine bacterial virulence (7), although another group demonstrated that platelet eluates from *H. pylori*–positive ITP patients that reacted with glycoprotein IIb/IIIa (GPIIb/IIIa) or GPIb failed to recognize *H. pylori* antigens (8). Another potential mechanism is modulation of the host's immune system by *H. pylori* in a manner that promotes the emergence of autoreactive B cells (9). However, no significant difference between *H. pylori*–positive and *H. pylori*–negative individuals has been found for non-organ-specific autoantibody responses, such as anti-nuclear, anti-microsome, or anti-smooth muscle Abs (10). Despite these findings, the role of *H. pylori* infection in the pathogenesis of ITP remains obscure. These previous studies focused on anti-platelet Ab production in association with *H. pylori* infection, but potential effects of *H. pylori* infection on the platelet clearance process in ITP patients have not been assessed. In this study, to elucidate the mechanism responsible for platelet recovery in ITP patients after the successful eradication of *H. pylori*, we conducted a prospective study in which factors potentially associated with the pathogenic processes of ITP, i.e., autoimmune responses to the major platelet antigen GPIIb/IIIa, parameters associated with platelet turnover, and the phenotypic and functional properties of phagocytes, were serially measured in ITP patients who were treated with a standard eradication regimen, irrespective of their *H. pylori* infection status.

Nonstandard abbreviations used: CagA, cytotoxin-associated gene A; FcγRIIB, Fcγ receptor IIB; GPIIb/IIIa, glycoprotein IIb/IIIa; ITP, immune thrombocytopenia purpura; RES, reticuloendothelial system; TPO, thrombopoietin.

Conflict of interest: The authors have declared that no conflict of interest exists.

Citation for this article: *J. Clin. Invest.* **118**:2939–2949 (2008). doi:10.1172/JCI34496.